processes

MDPI

Article

Derivation and Verification of Gaussian Terrain Wake Model Based on Wind Field Experiment

Wei Liu [1,2], Xiaoxun Zhu [3], Kaike Wang [2], Xiaoxia Gao [3,*], Shaohai Zhang [3,*], Lijiang Dong [1], Zeqi Shi [2], Hongkun Lu [3,4] and Jie Zhou [1]

1 Xinjiang Xinneng Group Urumqi Electric Power Construction and Commissioning Institute, Urumqi 830011, China
2 State Grid Xinjiang Company Limited Electric Power Research Institute, Urumqi 830013, China
3 Department of Power Engineering, North China Electric Power University (Baoding), Baoding 071003, China
4 Beijing Huazhidian Technology Co., Ltd., Beijing 102401, China
* Correspondence: gaoxiaoxia@ncepu.edu.cn (X.G.); zhangshaohaihai@outlook.com (S.Z.)

Abstract: Aiming at the problem where the current engineering wake model does not describe the wind speed distribution of the wake in the complex terrain wind farm completely, based on the three-dimensional full wake model (3DJGF wake model), this paper proposed a wake model that can predict the three-dimensional wind speed distribution of the entire wake region in the complex wind farm, taking into account the Coanda effect, wind shear effect, and wake subsidence under the Gaussian terrain. Two types of Doppler lidar were used to conduct wind field experiments, and the inflow wind profile and three-dimensional expansion of the wake downstream of the wind turbine on the Gaussian terrain were measured. The experimental results showed that the wake centerline and terrain curve showed similar variation characteristics, and the near wake profile was similar to a super-Gaussian shape (asymmetric super-Gaussian shape) under low-wind-speed conditions, while the near wake profile presented a bimodal shape (asymmetric bimodal shape) under high-wind-speed conditions. The predicted profiles of the Gaussian terrain wake model were compared with the experimental data and the three typical wake models. The comparison results showed that the newly proposed Gaussian terrain wake model fit well with the experimental data in both near wake and far wake regions, and it had better performance in predicting the wake speed of the Gaussian terrain wind farm than the other three wake models. It can effectively predict the three-dimensional velocity distribution in the whole wake region of complex terrain.

Keywords: wind field experiment; wake model; Gaussian terrain; Coanda effect; lidar

Citation: Liu, W.; Zhu, X.; Wang, K.; Gao, X.; Zhang, S.; Dong, L.; Shi, Z.; Lu, H.; Zhou, J. Derivation and Verification of Gaussian Terrain Wake Model Based on Wind Field Experiment. *Processes* **2022**, *10*, 2731. https://doi.org/10.3390/pr10122731

Academic Editor: Davide Papurello

Received: 9 November 2022
Accepted: 12 December 2022
Published: 17 December 2022

1. Introduction

Wind energy is one of the cleanest renewable energy sources and has abundant reserves, so countries pay great attention to the development of wind energy [1]. Flat terrain is the best site for onshore wind farms, allowing full use of wind resources without the influence of terrain and obstacles, and wind farms are less expensive to install and maintain in such terrain. However, with the decreasing resources of many flat terrains, more and more wind turbines are installed in relatively complex terrains [2,3]. Compared to wind farms on flat terrain, the wind flow over complex terrain is greatly disturbed by terrain variations and soil roughness, thus changing the wind potential at the rotor hub height and making the flow field variations more complex.

The qualitative analysis of the wake in complex terrain has been carried out mainly through wind tunnel experiments [4–6] and wind field experiments [7–10]. Lange et al. [11] studied the flow field of a large model of the Bolund Peninsula in a wind tunnel laboratory and found that the mean wind, wind shear, and turbulence levels are sensitive to changes in terrain, and that small changes in terrain can lead to changes in wind flow, which not only affects the power performance of wind turbines, but also affects the service life

and maintenance costs. Hyvarinen et al. [12] conducted a wind tunnel experiment to study the wake development on a sinusoidal hill with a wind turbine placed on a ridge, and their results showed that the downward deflection of the wake and the turbulent kinetic energy of hilly terrain increased compared with those of flat terrain. The wind tunnel experiment can control the test conditions more accurately, such as the pressure, temperature, and velocity of the air flow, but it is influenced by the wall effect and cannot reach the changeable turbulence intensity and atmospheric environment of the actual wind field. Therefore, many scholars have studied the wake distribution characteristics under complex terrain through on-site observation. Hansen et al. [13] analyzed the wake characteristics of wind turbines in complex terrain based on SCADA data from wind farm field tests, and their analysis showed that in very complex terrain, the wake often has a distortion effect. Menke et al. [14] analyzed the wake of a single wind turbine in complex terrain by using LIDAR measurements, and their results showed that atmospheric stability has a strong influence on the wake propagation in the vertical direction. The above research on wakes over complex terrain is limited to qualitative analysis, which can only roughly understand the characteristics of wake changes and cannot be applied to layout optimization and control strategies of complex wind farms. Therefore, quantitative analysis of the wake is essential.

Quantitative analysis of the complex terrain wake is mainly based on numerical simulations [15–17] as well as analytical modeling [18–20]. Kuo et al. [21] proposed an algorithm combining computational fluid dynamics (CFD) and mixed-integer programming (MIP) to optimize the layout on complex terrain. Liu et al. [22] studied two superposition methods to predict the wind turbine wake on complex terrain through large eddy simulations, and their results showed that the superposition method along the central streamline of the wind turbine has a better prediction effect. Li et al. [16] used large eddy simulations to study the wake distribution of wind turbines installed on complex terrain, and found that the shape of complex terrain determines the impact of ground roughness and atmospheric stratification on the wind turbine wake. The above numerical simulation methods have high computational accuracy, but the applicability of high-fidelity simulation results are more limited and computationally expensive [19,20], and cannot be applied to actual wind farms, so the analytical wake model with low computational cost and high computational accuracy has become a hot research topic. Feng et al. [23] introduced topographic features into the Jensen wake model. The Jensen wake model with topographic features can optimize the layout of two-dimensional wind farms on the Gauss Mountain. However, the Jensen wake model assumes that the wake is linearly related to the downstream distance, which is not in line with reality. Therefore, the layout optimization system based on the Jensen wake model still has large defects. Ibrahim et al. [18] proposed an engineering wake model consisting of wake width and wake wind speed. This model is based on momentum theory and considers two-dimensional mountain slope acceleration, but it can only predict the wake speed in the horizontal direction, which is still very limited for the wake analysis of wind farms. Brogna et al. [24] proposed a new wake engineering model by superimposing a Gaussian shape on the top of the complex terrain flow field and assuming that the centerline of the wind turbine wake follows the streamline of the complex terrain flow field. However, the wake velocity distribution in the vertical direction predicted by the model is in a symmetrical Gaussian shape, which is quite different from the wake distribution of the actual wind field. Tian et al. [25] quantified the wake characteristics of wind turbines on two-dimensional Gaussian hills with different slopes by means of an actuator disk model, and used the parameters of complex terrain to modify the traditional flat terrain. A new model based on a local acceleration factor and a simulated wind turbine wake velocity calculation was proposed. The above wake model for complex terrain does not take into account the wind shear effect, and the influence of the wind shear effect on the wake distribution cannot be ignored [26–28], especially in the vertical wake distribution. In order to solve this problem, Gao et al. [29] introduced the Coanda effect into the wake model, considered the effect of wind shear, modified the wind speed distribution in the

vertical direction, and proposed a complex terrain wake model suitable for the far wake region. However, the model does not fully describe the velocity distribution of the whole wake region, and it ignores the distribution characteristics of the near wake. However, in actual wind farms, with the continuous reduction in ground resources, the spacing between many wind turbines is less than $4D$ [30], which means that many downstream wind turbines are affected by the near wake generated by upstream wind turbines, so it is necessary to quantify the near wake.

Based on these, a new tail flow model for Gaussian terrain is proposed in this paper, which can predict the three-dimensional velocity distribution characteristics of the entire wake region of a wind turbine on a Gaussian-shaped hill. The wind shear effect and the Coanda effect on the wake of a wind turbine on a Gaussian terrain are taken into account, and the wind field experiments on complex terrain are conducted to validate the proposed wake model.

The innovations and contributions of this paper are as follows:

1. The Gaussian terrain wake model proposed in this paper considers the influence of the Coanda effect and wind shear effect, and can accurately predict the three-dimensional wake distribution of wind farms in complex terrain;
2. Unlike previous engineering wake models, the newly proposed Gaussian terrain wake model takes into account the velocity distribution characteristics of the whole wake region of wind farms in complex terrain, which includes not only the far wake region, but also the near wake region;
3. Two high-precision lidars are used to capture the three-dimensional distribution characteristics of free flow and wake, and the captured data are more complete and reliable than the data measured by the wind measuring mast;
4. The newly proposed Gaussian terrain wake model can effectively predict the three-dimensional wind speed distribution of the whole wake field in complex terrain, and the calculation cost is far lower than that of the high-fidelity model, which can be applied to the actual wind field and provide a reference for the optimization of the wind farm layout.

2. Gaussian Terrain Wake Model Derivation

The basic idea of the derivation of the Gaussian terrain wake model is to consider the Coanda effect on the basis of the traditional engineering wake model, then calculate the wake sinking height, and finally correct the three-dimensional full wake model (3DJGF wake model).

2.1. The 3DJGF Wake Model

There are many wake models for flat-terrain wind farms, but in order to make the Gaussian terrain wake model more comprehensive, this paper selects the 3DJGF wake model derived by Gao [31] that can describe the entire wake region as the benchmark wake model for deriving the Gaussian terrain wake model, and its expression is shown in Equation (1).

$$\begin{cases} u(x,y,z) = u_{\text{hub}}\left[\left(\frac{z+z_{\text{hub}}}{z_{\text{hub}}}\right)^{\alpha} - C\left(\frac{\mathrm{e}^{-\frac{(y+y_{\min})^2}{2\sigma_{\text{y}}^2}} + \mathrm{e}^{-\frac{(y-y_{\min})^2}{2\sigma_{\text{y}}^2}}}{2}\right)\right] \\ C = \frac{4ar_0{}^2}{\sqrt{2\pi}\sigma_z r_z}\mathrm{e}^{\frac{y_{\min}^2}{2\sigma_{\text{y}}^2}}\left(\frac{\mathrm{e}^{-\frac{(z+z_{\min})^2}{2\sigma_z^2}} + \mathrm{e}^{-\frac{(z-z_{\min})^2}{2\sigma_z^2}}}{2}\right) + \mathrm{e}^{\frac{y_{\min}^2}{2\sigma_{\text{y}}^2}}\frac{a\int_{-r_0}^{r_0}\left(\left(\frac{z+z_{\text{hub}}}{z_{\text{hub}}}\right)^{\alpha}-1\right)\mathrm{d}z}{r_z} \end{cases} \quad (1)$$

where u_{hub} is the incoming wind speed in front of the hub center, m/s; z_{hub} is the vertical height from the center of the hub to the ground, m; r_0 is the initial wake radius, m; r_{y} is the wake radius horizontally, m; r_z is the wake radius in the vertical direction, m; σ_{y} is the characteristic wake width in the horizontal direction; σ_{z} is the width of the characteristic

wake in the vertical direction; $y_{\min}$ is the distance from the Gaussian minimum to the center line of the wake horizontally; $z_{\min}$ is the distance from the Gaussian minimum to the center line of the wake vertically; a is an axial induction factor; α is the wind shear index, obtained from the incoming wind profile measured by the wind field.

Due to the properties of the Gaussian function, 2.81 standard deviations can reach a probability of 99% in each dimension, so it can be assumed that the characteristic width expression of the wake is as follows [31]:

$$\begin{cases} \sigma_y = r_y/[2.81(1 + c_1 e^{-c_2 x^2})] \\ \sigma_z = r_z/[2.81(1 + c_1 e^{-c_2 x^2})] \end{cases} \tag{2}$$

where c_1 and c_2 are parameters and are obtained by fitting the changing trend of the wake centerline.

The wake radii horizontally r_y and vertically r_z follow the linear hypothesis proposed by Jensen [32], which is expressed as follows:

$$\begin{cases} r_y = k_y x + r_0 \\ r_z = k_z x + r_0 \end{cases} \tag{3}$$

where k_y is the wake expansion coefficient in the horizontal direction; k_z is the wake expansion coefficient in the vertical direction. As the velocity of wake expansion is not the same horizontally and vertically, the expression of the wake expansion coefficient with anisotropy is used [33]. The expressions for the wake expansion coefficient horizontally k_y and the wake expansion coefficient vertically k_z are shown in Equation (4):

$$\begin{cases} k_y = 0.18265 C_T^{0.2566} I_0^{0.2808} \\ k_z = 0.243346 C_T^{0.4297} I_0^{0.4707} \end{cases} \tag{4}$$

where C_T is the thrust coefficient of the wind turbine, which is determined by the flow speed from the center of the hub; I_0 is the incoming turbulence intensity, which is obtained from the ratio of the standard deviation and the average wind speed within 10 min.

The initial wake radius r_0 can be determined by Equation (5) [34]:

$$r_0 = D\sqrt{(1-a)/(1-2a)}/2 \tag{5}$$

In Equation (5), D is the diameter of the wind turbine.

The axial inducible factor expression a is as follows:

$$a = (1 - \sqrt{1 - C_T})/2 \tag{6}$$

Figure 1 shows a schematic diagram of a double-Gaussian function. The expression for the distance from the Gaussian minimum to the center line of the wake horizontally and the distance from the Gaussian minimum to the center line of the wake vertically can be obtained from the characteristics of the double-Gaussian function, as shown in Equation (7):

$$\begin{cases} y_{\min} = r_y - 2.81\sigma_y = 2.81 c_1 e^{-c_2 x^2} \sigma_y \\ z_{\min} = r_z - 2.81\sigma_z = 2.81 c_1 e^{-c_2 x^2} \sigma_z \end{cases} \tag{7}$$

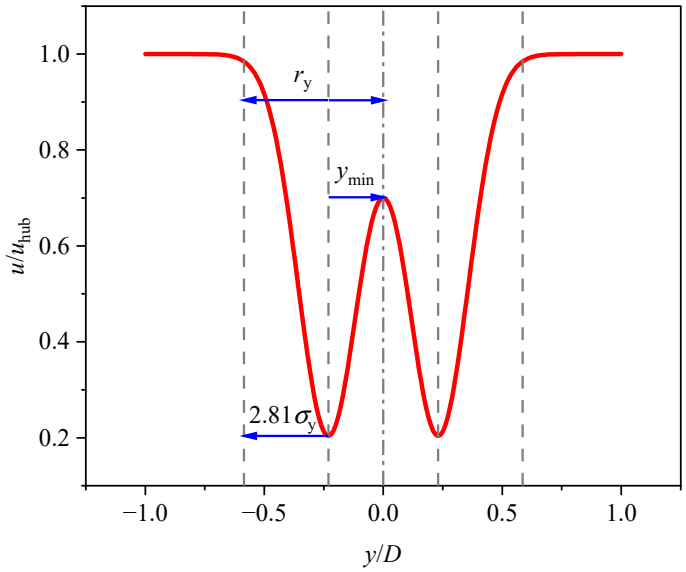

Figure 1. Schematic diagram of a double-Gaussian function.

2.2. Coanda Effect

The Coanda effect, also known as the wall effect, refers to the tendency where when the fluid encounters a convex surface, the fluid deviates from the original flow direction and flows with the convex surface [29]. The Coanda effect is caused by the sudden change in terrain, which leads to the pressure difference on both sides of the fluid. Under the effect of the pressure difference, the fluid shifts from the high-pressure side to the low-pressure side, and finally achieves a stable flow state of the attached wall.

Wind turbines installed on complex terrain are affected by the Coanda effect. In the actual wind farm, there are inevitably prominent ridges. When the wind flows through the windward sides of the ridges, the flow rate of the near-ground-side gas decreases, the pressure increases due to the gas being obstructed, and the near-ground-side wind flows to the far side, so the fluid streamlines have an upward trend. When the wind flows through the leeward sides of the ridges, there is a wind acceleration effect, which leads to an increase in the velocity near the ground and a decrease in the pressure, and the wind on the far side flows toward the near ground side, so the streamlines of the fluid on the leeward sides have a downward trend. On the windward sides of the ridges, the streamlines of the fluid are upward, and on the leeward sides, the streamlines of the fluid are downward, which forms the Coanda effect, as shown in Figure 2.

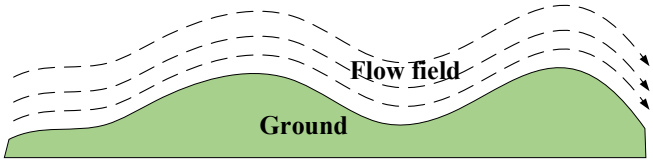

Figure 2. Schematic diagram of the Coanda effect.

2.3. Gaussian Terrain Wake Model

The 3DJGF wake model does not take into account the influence of terrain changes on the wake, believing that the wake center is on the hub height line, while in the actual complex terrain wind farm, the wake center will change with the change in terrain, and the change in the wake center is generally reflected in the wake sinking in the vertical direction. This article takes the Gaussian-shaped ground that is more common in wind farms as an example. From the Coanda effect, when the terrain behind the wind turbine falls, the wake will also sink with the terrain, assuming that the vertical height of the Gaussian-shaped

ground where the wind turbine is h and the sinking height of the wake center is Δh, as shown in Figure 3.

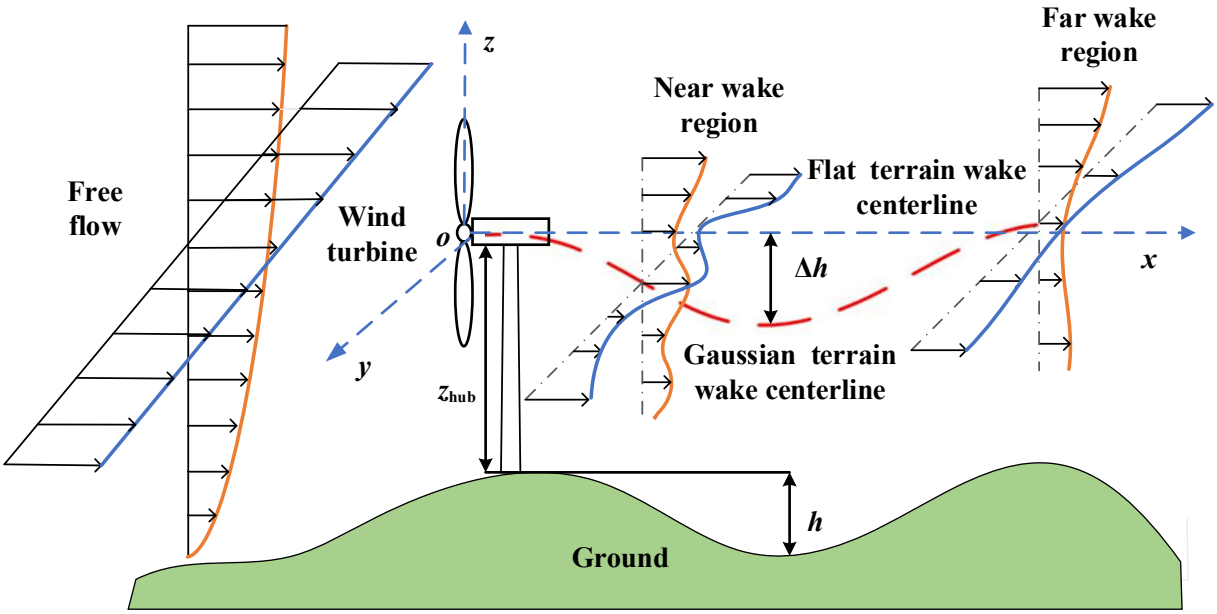

Figure 3. Schematic diagram of wind turbine wake center sinking on Gaussian terrain.

Taking the center of the wind turbine hub as the coordinate origin, the Gaussian terrain surface expression is as follows:

$$f(x) = h\left(\mathrm{e}^{-\frac{x^2}{2\sigma^2}} - 1\right) - z_{\mathrm{hub}} \tag{8}$$

where σ is the standard deviation, obtained by fitting the Gaussian terrain surface.

Then, the wake center sink height Δh expression is:

$$\Delta h = -z_{\mathrm{hub}} - f(x) = h\left(1 - \mathrm{e}^{-\frac{x^2}{2\sigma^2}}\right) \tag{9}$$

Combining Equations (1)–(9) obtains a Gaussian terrain wake model, the expression of which is shown in Equation (10):

$$\begin{cases} u(x,y,z) = u_{\mathrm{hub}}\left[\left(\frac{z+z_{\mathrm{hub}}+h-h\mathrm{e}^{-\frac{x^2}{2\sigma^2}}}{z_{\mathrm{hub}}}\right)^{\alpha} - C_{\mathrm{h}}\left(\frac{\mathrm{e}^{-\frac{(y+y_{\min})^2}{2\sigma_y^2}} + \mathrm{e}^{-\frac{(y-y_{\min})^2}{2\sigma_y^2}}}{2}\right)\right] \\ C_{\mathrm{h}} = \frac{4ar_0{}^2}{\sqrt{2\pi}\sigma_z r_z}\mathrm{e}^{\frac{y_{\min}^2}{2\sigma_y^2}}\left(\frac{\mathrm{e}^{-\frac{(z+z_{\min}+h-h\mathrm{e}^{-\frac{x^2}{2\sigma^2}})^2}{2\sigma_z^2}} + \mathrm{e}^{-\frac{(z-z_{\min}+h-h\mathrm{e}^{-\frac{x^2}{2\sigma^2}})^2}{2\sigma_z^2}}}{2}\right) + \mathrm{e}^{\frac{y_{\min}^2}{2\sigma_y^2}}\frac{a\int_{-r_0}^{r_0}\left(\left(\frac{z+z_{\mathrm{hub}}+h-h\mathrm{e}^{-\frac{x^2}{2\sigma^2}}}{z_{\mathrm{hub}}}\right)^{\alpha}-1\right)\mathrm{d}z}{r_z} \end{cases} \tag{10}$$

3. Wind Field Experiments

From January to April 2019, our team conducted wind farm measurements at an onshore wind farm with complex terrain in northern Hebei Province. The wind turbine to the north of the wind farm is located on a Gaussian hill, which is one of the typical installation methods for wind turbines in complex terrain. Therefore, the wind turbine wake expansion process at this location can be measured and used to validate the Gaussian terrain wake model. Two models, the W3D6000 (a ground-based vertical lidar) and WP350 (a ground-based vertical lidar), were used in wind field experiments, and WP350 was

used to measure the wind speed, wind direction, turbulence intensity, and wind profile of incoming flow. The W3D6000 has both RHI and PPI scanning modes, where the RHI mode (fixed azimuth and adjustable elevation angle) can be used to measure the vertical wind profile of the wind turbine wake, and the PPI mode (fixed elevation angle and adjustable azimuth) can be used to measure the horizontal wind profile of the wake. A schematic of the lidar measurement is shown in Figure 4.

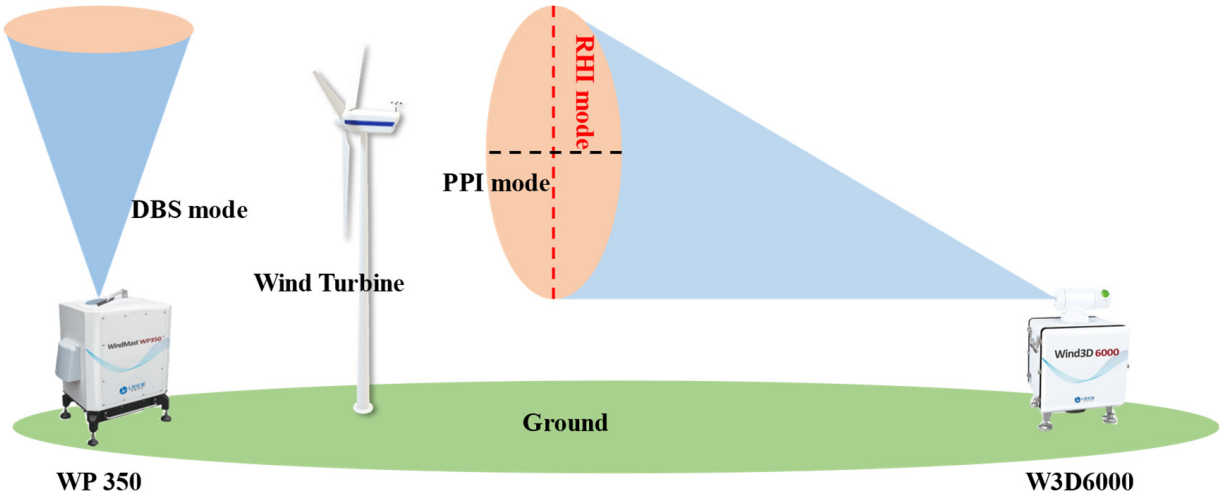

Figure 4. Schematic diagram of two types of lidar measurement.

According to the wind tower data analysis, the main wind direction of the wind farm is the northwest wind. Therefore, in order to measure a more complete wake distribution, WP350 is arranged in the northwest direction of the 3-2 wind turbine, 160 m away from the 3-2 wind turbine; the W3D6000 is arranged in the southeast direction of the 3-2 wind turbine, 1275 m away from the 3-2 wind turbine; the height difference between the center of the wind turbine hub and the W3D6000 is 72 m. The exact locations of the lidar and wind turbines are shown in Figure 5. The yellow lines in Figure 5 represent the contour lines, and the yellow pushpins represent the positions of the wind turbines.

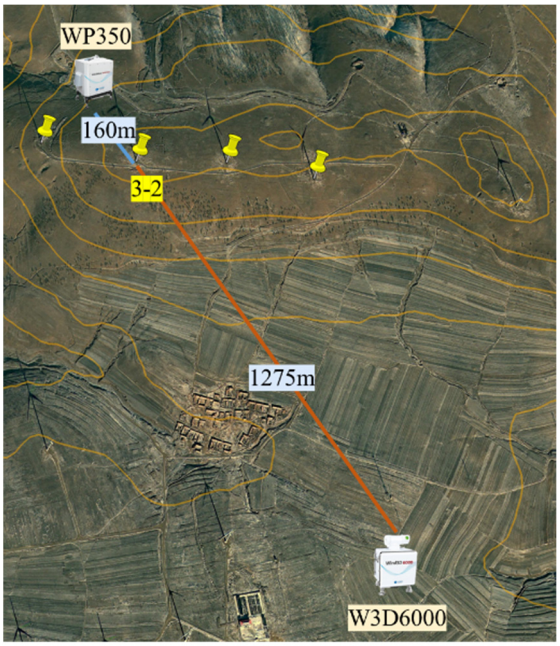

Figure 5. Layout of lidars.

4. Results and Discussion

In order to demonstrate the effectiveness of the Gaussian terrain wake model proposed in this paper, the predicted horizontal and vertical profiles of the model were validated; three recently proposed wake models were selected for comparison to show the improvement of model accuracy. The three wake models were the 3DJG-H model (complex terrain wake model) proposed by Gao et al. [29], 3DJGF model (flat terrain wake model) proposed by Gao et al. [31], and 3DEG model (flat terrain wake model) proposed by He et al. [33].

The 3-2 wind turbine hub center height $z_{\mathrm{hub}} = 65$ m, the Gaussian-shaped peak height $h = 72$ m, the standard deviation $\sigma = 5$ of the fitted Gaussian terrain surface function, and the corresponding variation curve of wake sink height Δh with downstream distance x are shown in Figure 6.

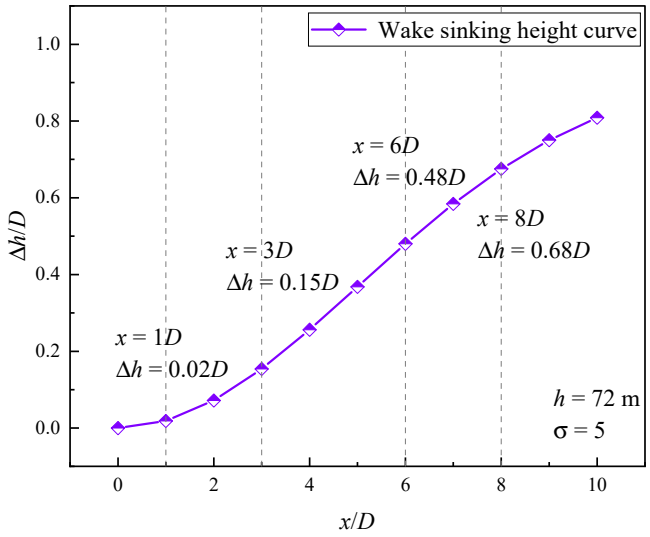

Figure 6. Wake sinking height curve.

4.1. Horizontal Profile Verification

The wind velocity distribution of the wake flow in the horizontal direction downstream of the wind turbine can be obtained by the PPI mode of W3D6000, as shown in Figure 7. It can be seen that the wake of the 3-2 wind turbine is obviously complete and not disturbed by the wake of other wind turbines, which is suitable for analyzing the extended characteristics of the wake in the horizontal direction.

The incoming turbulence intensity $I_0 = 0.08$ and the incoming wind speed $u_{\mathrm{hub}} = 5.9$ m/s at the hub center correspond to a thrust coefficient $C_{\mathrm{T}} = 0.85$ measured by WP350 for 10 min. In this paper, horizontal profile wake data from four locations downstream of the wind turbine ($x = 1D$, $x = 3D$, $x = 6D$, and $x = 8D$) were selected to verify the validity of the Gaussian terrain wake model in the horizontal direction, as shown in Figure 8. From the comparison results, the prediction accuracy of the Gaussian terrain wake model is better than those of the other three wake models on the whole. However, it is worth noting that at $x = 1D$, the prediction error of the Gaussian terrain wake model is higher than those of several other downstream locations, especially at the center of the wake, which is mainly due to the fact that the Gaussian terrain wake model is based on the double-Gaussian. In addition, the prediction profile at the near wake shows a bimodal shape, while the incoming wind speed in this experiment is only 5.9 m/s, which corresponds to a large thrust coefficient. Under this small-wind-speed condition, the near wake profile resembles a super-Gaussian shape, which is consistent with the experimental results of Blondel et al. [30], so the Gaussian terrain wake model is slightly less effective in predicting the near wake under small-wind-speed conditions. The 3DJG-H wake model is only applicable to the far wake region, so the prediction accuracy of the model in the near wake region is lower than that of the Gaussian terrain wake model. However, because the 3DJG-H wake model considers the influence of terrain on the wake distribution, the prediction accuracy in the far wake region is

acceptable. The 3DJGF wake model does not take into account the settlement of the wake, so its overall prediction accuracy is poor. As the wake sinking phenomenon becomes more obvious with the increase in the downstream distance, the prediction accuracy of the 3DJGF wake model shows a negative correlation trend with the downstream distance. The 3DEG wake model does not consider the influence of wake sinking, so its prediction results are not ideal. Due to the limitation of its mathematical expression, the 3DEG wake model cannot predict the distribution of the near wake.

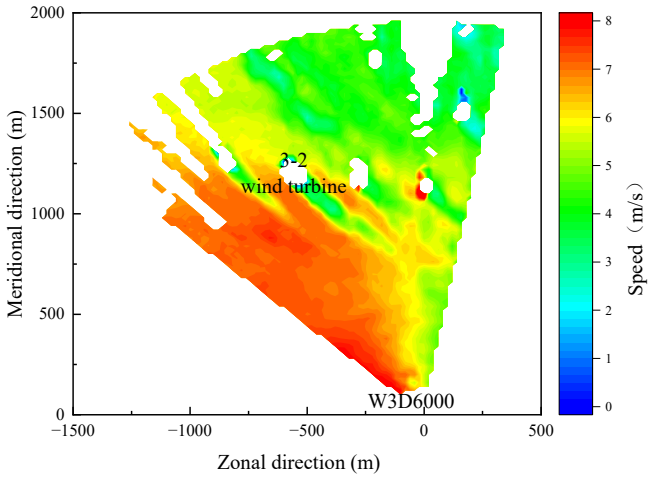

Figure 7. Cloud image of 3-2 wind turbine horizontal profile measured by W3D6000.

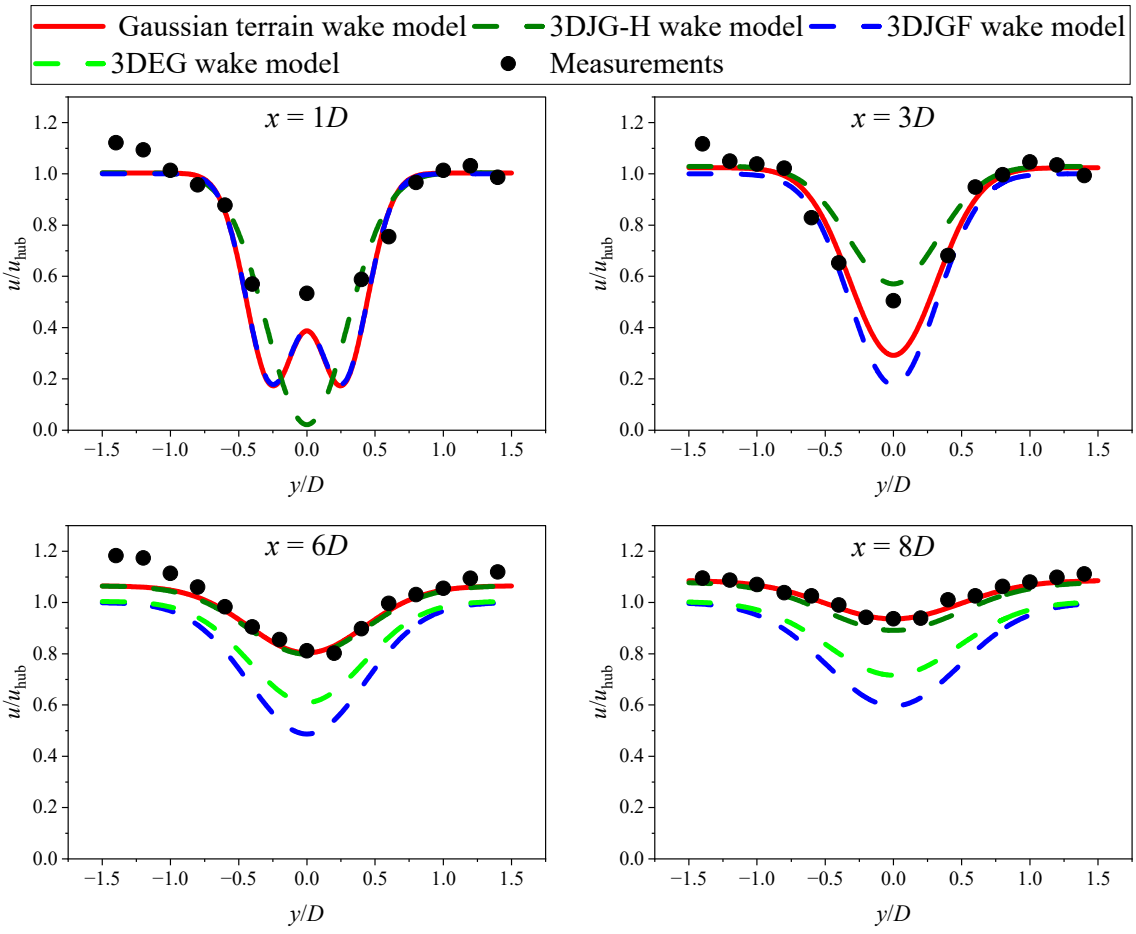

Figure 8. Comparison results of horizontal profiles at four downstream locations.

4.2. Vertical Profile Verification

In order to verify the accuracy of the Gaussian terrain wake model in the vertical direction, the vertical profile cloud map of the 3-2 wind turbine captured by the RHI mode of the W3D6000 LiDAR was selected in this paper, as shown in Figure 9. The cloud map is based on the W3D6000 LiDAR as the coordinate origin, the vertical direction as the vertical axis, and the longitude direction as the horizontal axis, and the hub center coordinates of the 3-2 wind turbine were (1275, 137).

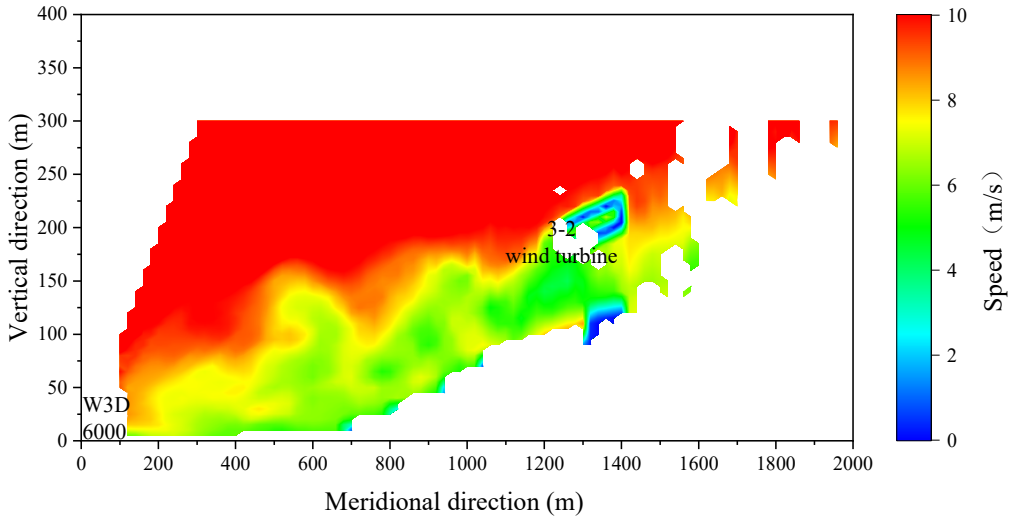

Figure 9. Cloud image of 3-2 wind turbine vertical profile measured by W3D6000.

The incoming turbulence intensity $I_0 = 0.11$, the incoming wind speed $u_{\text{hub}} = 9$ m/s at the hub center, the corresponding thrust coefficient $C_T = 0.749$, and the wind shear index $a = 0.14$ were measured by WP350 for 10 min.

As with the horizontal profiles, vertical profile wake data from four locations downstream of the wind turbine ($x = 1D$, $x = 3D$, $x = 6D$, and $x = 8D$) were selected to verify the validity of the Gaussian terrain wake model in the vertical direction, as shown in Figure 10. From the measured wake profile data, it can be seen that at $x = 1D$, the vertical wake wind speed distribution resembles an asymmetric bimodal shape, while the measured wind speed profiles at the other three downstream locations resemble an asymmetric unimodal shape. From the comparison results of the vertical profiles, the prediction effect of the Gaussian terrain wake model in the whole wake region is better than those of the other three wake models. It is worth noting that the Gaussian topography model has a large error in predicting the velocity on the centerline of the wake at $x = 1D$, which obviously underestimates the wake velocity. This may be due to the fact that $x = 1D$ is closer to the wind turbine and the wake center is more seriously influenced by the wind turbine nacelle, plus the turbulence intensity changes are more complicated near the wake, especially near the wake centerline, so it leads to a larger error in predicting the wake center. At $x = 3D$, the predicted profile of the Gaussian terrain wake model is asymmetric single-peaked, which is consistent with the measured wake profile. Similar to $x = 3D$, the prediction error of the Gaussian terrain wake model is larger near the wake center because $x = 3D$ is at the boundary between the near and far wake regions, and the turbulence variation on the wake centerline is more complex than the turbulence intensity variation at other locations. However, the newly proposed Gaussian terrain wake model uses a simple turbulence intensity model, which does not accurately predict the turbulence intensity change on the centerline, resulting in a slightly larger prediction error at the center of the wake than at other vertical locations. In the other two downstream locations, the predicted curves of the Gaussian terrain wake model and the measured profiles are in good agreement, and their prediction errors are both small. The 3DJG-H wake model is only applicable to the far wake region, so its prediction accuracy for the wake at $x = 3D$,

$x = 6D$, and $x = 8D$ is good, while the prediction accuracy at $x = 1D$ is poor, which seriously underestimates the wind speed near the wake center. The prediction profile of the 3DJGF wake model at $x = 1D$ is not very different from that of the Gaussian terrain wake model, both of which are asymmetric bimodal, and both of which are in good agreement with the measured profile. This is mainly because at $x = 1D$, the terrain changes little, and the wake sinking phenomenon is not obvious, so the prediction results of the 3DJGF wake model and the Gaussian terrain wake model are similar. Meanwhile, at the other three downstream locations, because the 3DJGF wake model does not consider the wake settlement, the prediction error is large. With the increase in the downstream distance, the terrain change also increases, and the wake sinking phenomenon is more and more obvious. The 3DEG wake model does not take into account the influence of the terrain on the wake sinking, so the prediction effect on the wake speed is not ideal.

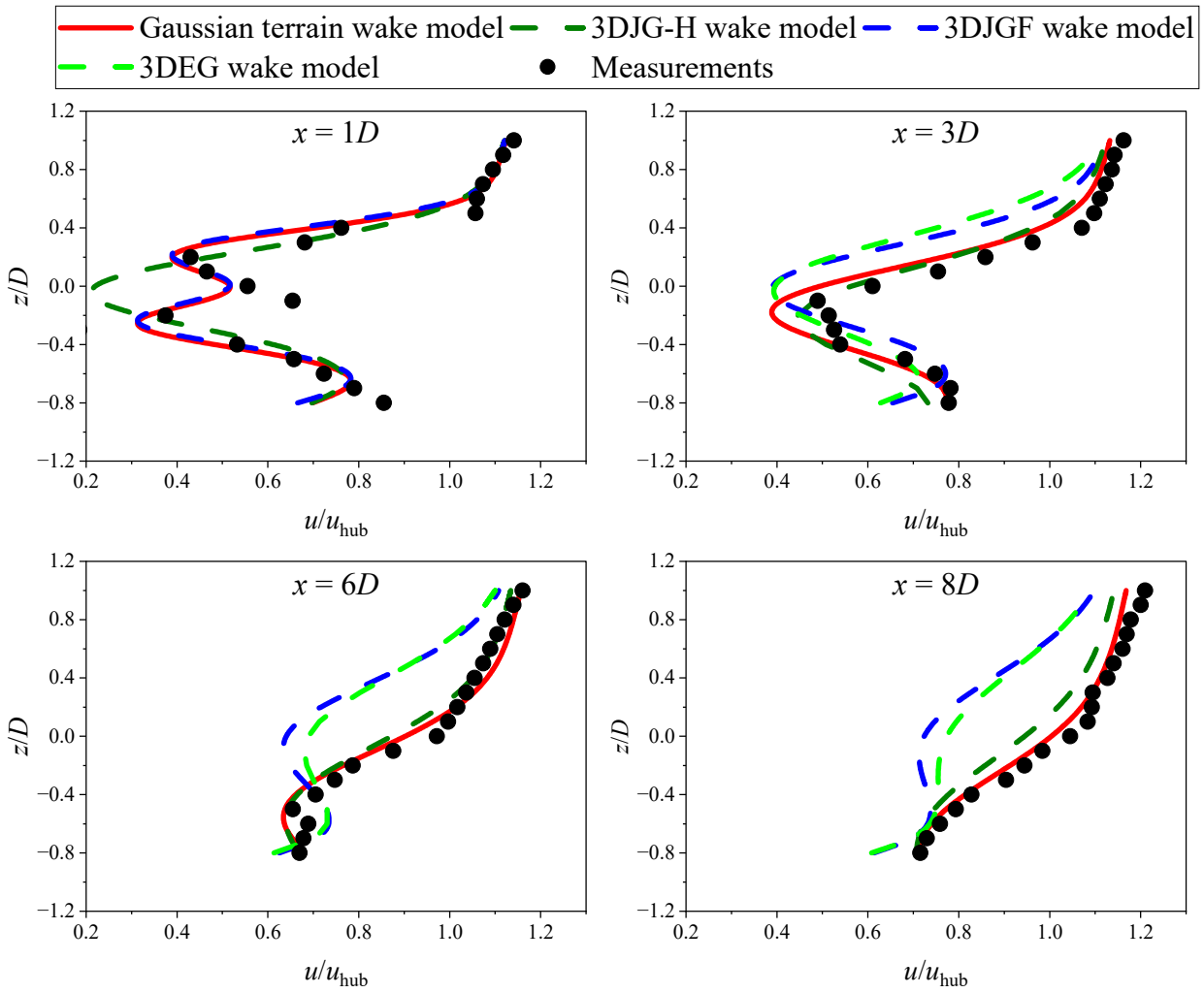

Figure 10. Comparison results of vertical profiles at four downstream locations.

From the above analysis, it can be obtained that the Gaussian terrain wake model has good prediction results at the remaining downstream locations except for the large prediction error near the wake centerline of the near wake, and the prediction accuracy is higher than those of the other three wake models, which can effectively predict the three-dimensional distribution characteristics of the wake generated by wind turbines on Gaussian terrain.

5. Conclusions

Based on the 3DJGF wake model, this paper proposes a Gaussian terrain wake model considering the Coanda effect, the wind shear effect, and the distribution characteristics of the entire wake. At the same time, the wind field experiment using two lidars to verify the accuracy of the model is summarized as follows:

(1) Due to the influence of wind shear in the vertical profile, the vertical profile of the wake presents an asymmetric shape;
(2) Affected by the Coanda effect of Gaussian topography, the height of the center of the wake changes with the change in the terrain, and shows similar change characteristics to the terrain curve;
(3) From the wake profile data measured by the wind field, it can be seen that under small-wind-speed conditions (large thrust coefficient), the near wake profile is similar to the super-Gaussian shape, while under the condition of larger wind speeds (small thrust coefficient), the near wake profile shows a bimodal shape.
(4) The newly proposed Gaussian terrain wake model is compared with the measured data and the three wake models, the prediction results and experimental data of the Gaussian terrain wake model fit well in both horizontal and vertical directions, and the prediction accuracy greatly improves compared with the other three wake models;
(5) The newly proposed Gaussian terrain wake model can accurately predict the three-dimensional wake distribution downstream of wind turbines, which can provide a reference for wind resource evaluation and microscopic site selection of wind farms with complex terrain.

Author Contributions: Conceptualization, W.L. and X.Z.; methodology, K.W.; supervisor, X.G.; validation, S.Z.; formal analysis, L.D.; investigation, Z.S.; resources, H.L.; data curation, J.Z. All authors have read and agreed to the published version of the manuscript.

Funding: This research was funded by National Natural Science Foundation of China: No. 52076081; the Fundamental Research Funds for the Central Universities: No. 2020MS107; the Research Institute for Sustainable Urban Development (RISUD) with account number of BBW8 of The Hong Kong Polytechnic University: No. 1-BBW8; the state Grid Xinjiang Company Limited Electric Power Research Institute science and technology project of the development of customized wind power prediction system under terrain wake coupling: No. SGXJXNOOTSJS2200142; Research project of state perception and fault diagnosis technology for multi field coupling vibration of hydropower units: No. SGXJXN00TSJS2200143; Post-graduate's Innovation Fund Project of Hebei Province: No. CXZZSS2023192.

Data Availability Statement: Not applicable.

Acknowledgments: The APC was funded by Xiaoxia Gao.

Conflicts of Interest: The authors declare no conflict of interest.

References

1. Song, D.; Tu, Y.; Wang, L.; Jin, F.; Li, Z.; Huang, C.; Xia, E.; Rizk-Allah, R.M.; Yang, J.; Su, M.; et al. Coordinated optimization on energy capture and torque fluctuation of wind turbines via variable weight NMPC with fuzzy regulator. *Appl. Energy* **2022**, *312*, 118821. [CrossRef]
2. Alfredsson, P.H.; Segalini, A. *Introduction Wind Farms in Complex Terrains: An Introduction*; The Royal Society Publishing: London, UK, 2017; p. 20160096. [CrossRef] [PubMed]
3. Feng, J.; Shen, W.Z.; Li, Y. An optimization framework for wind farm design in complex terrain. *Appl. Sci.* **2018**, *8*, 2053. [CrossRef]
4. Bastankhah, M.; Porte-Agel, F. Wind tunnel study of the wind turbine interaction with a boundary-layer flow: Upwind region, turbine performance, and wake region. *Phys. Fluids* **2017**, *29*, 065105. [CrossRef]
5. Dar, A.S.; Porte-Agel, F. Wind turbine wakes on escarpments: A wind-tunnel study. *Renew. Energy* **2022**, *181*, 1258–1275. [CrossRef]
6. Huang, G.; Zhang, S.; Yan, B.; Yang, Q.; Zhou, X.; Ishihara, T. Thrust-matched optimization of blades for the reduced-scale wind tunnel tests of wind turbine wakes. *J. Wind. Eng. Ind. Aerodyn.* **2022**, *228*, 105113. [CrossRef]
7. Zhao, F.; Gao, Y.; Wang, T.; Yuan, J.; Gao, X. Experimental Study on Wake Evolution of a 1.5 MW Wind Turbine in a Complex Terrain Wind Farm Based on LiDAR Measurements. *Sustainability* **2020**, *12*, 2467. [CrossRef]

8. Sun, H.; Gao, X.; Yang, H. Experimental study on wind speeds in a complex-terrain wind farm and analysis of wake effects. *Appl. Energy* **2020**, *272*, 115215. [CrossRef]
9. Pacheco de Sá Sarmiento, F.I.; Goes Oliveira, J.L.; Passos, J.C. Impact of atmospheric stability, wake effect and topography on power production at complex-terrain wind farm. *Energy* **2022**, *239*, 122211. [CrossRef]
10. Wang, Q.; Luo, K.; Wu, C.; Mu, Y.; Tan, J.; Fan, J. Diurnal impact of atmospheric stability on inter-farm wake and power generation efficiency at neighboring onshore wind farms in complex terrain. *Energy Convers. Manag.* **2022**, *267*, 115897. [CrossRef]
11. Lange, J.; Mann, J.; Berg, J.; Parvu, D.; Kilpatrick, R.; Costache, A.; Chowdhury, J.; Siddiqui, K.; Hangan, H. For wind turbines in complex terrain, the devil is in the detail. *Environ. Res. Lett.* **2017**, *12*, 094020. [CrossRef]
12. Hyvärinen, A.; Lacagnina, G.; Segalini, A. A wind-tunnel study of the wake development behind wind turbines over sinusoidal hills. *Wind. Energy* **2018**, *21*, 605–617. [CrossRef]
13. Hansen, K.S.; Larsen, G.C.; Menke, R.; Vasiljevic, N.; Angelou, N.; Feng, J.; Zhu, W.J.; Vignaroli, A.; Liu, W.; Xu, C.; et al. *Wind Turbine Wake Measurement in Complex Terrain*; IOP Publishing: Munich, Germany, 2016; p. 032013. [CrossRef]
14. Menke, R.; Vasiljević, N.; Hansen, K.S.; Hahmann, A.N.; Mann, J. Does the wind turbine wake follow the topography? A multi-lidar study in complex terrain. *Wind. Energy Sci.* **2018**, *3*, 681–691. [CrossRef]
15. Stevens, R.; Gayme, D.F.; Meneveau, C. Effects of turbine spacing on the power output of extended wind-farms. *Wind. Energy* **2016**, *19*, 359–370. [CrossRef]
16. Li, T.; Liu, Z.; Wang, H.; Bian, W.; Yang, Q. Large eddy simulation for the effects of ground roughness and atmospheric stratification on the wake characteristics of wind turbines mounted on complex terrains. *Energy Convers. Manag.* **2022**, *268*, 115977. [CrossRef]
17. Wang, Q.; Luo, K.; Wu, C.; Zhu, Z.; Fan, J. Mesoscale simulations of a real onshore wind power base in complex terrain: Wind farm wake behavior and power production. *Energy* **2022**, *241*, 122873. [CrossRef]
18. Ibrahim, O.M.; Yoshida, S.; Hamasaki, M.; Takada, A. Wind Turbine Wake Modeling in Accelerating Wind Field: A Preliminary Study on a Two-Dimensional Hill. *Fluids* **2019**, *4*, 153. [CrossRef]
19. Sun, H.; Gao, X.; Yang, H. Validations of three-dimensional wake models with the wind field measurements in complex terrain. *Energy* **2019**, *189*, 116213. [CrossRef]
20. Liu, H.; Fu, J.; Liang, Z.; Liang, Z.; Zhang, Y.; Xiao, Z. A simple method of fast evaluating full-field wake velocities for arbitrary wind turbine arrays on complex terrains. *Renew. Energy* **2022**, *201*, 961–976. [CrossRef]
21. Kuo, J.Y.J.; Romero, D.A.; Beck, J.C.; Amon, C.H. Wind farm layout optimization on complex terrains—Integrating a CFD wake model with mixed-integer programming. *Appl. Energy* **2016**, *178*, 404–414. [CrossRef]
22. Liu, Z.; Ishihara, T. Large eddy simulations of wind-turbine wakes in typical complex topographies. *Wind. Energy* **2020**, *24*, 857–886. [CrossRef]
23. Feng, J.; Shen, W.Z. *Wind Farm Layout Optimization in Complex Terrain: A Preliminary Study on a Gaussian Hill*; IOP Publishing; Tech Univ Denmark: Copenhagen, Denmark, 2014; p. 012146. [CrossRef]
24. Brogna, R.; Feng, J.; Sørensen, J.N.; Shen, W.Z.; Porté-Agel, F. A new wake model and comparison of eight algorithms for layout optimization of wind farms in complex terrain. *Appl. Energy* **2020**, *259*, 114189. [CrossRef]
25. Tian, W.; Zheng, K.; Hu, H. Investigation of the wake propagation behind wind turbines over hilly terrain with different slope gradients. *J. Wind. Eng. Ind. Aerodyn.* **2021**, *215*, 104683. [CrossRef]
26. Chanprasert, W.; Sharma, R.N.; Cater, J.E.; Norris, S.E. Large Eddy Simulation of wind turbine wake interaction in directionally sheared inflows. *Renew. Energy* **2022**, *201*, 1096–1110. [CrossRef]
27. Abkar, M.; Porte-Agel, F.; Sorensen, J.N. Wind Turbine Wakes in Directionally Varying Wind Shears. *Prog. Turbul.* **2019**, *viii*, 311–316.
28. Li, L.; Hearst, R.J.; Ganapathisubramani, B. The Mean Velocity of the Near-Field of a Lab-Scale Wind Turbine in Tailored Turbulent Shear Flows. *Prog. Turbul.* **2019**, *viii*, 317–322.
29. Xiaoxia, G.; Luqing, L.; Shaohai, Z.; Xiaoxun, Z.; Haiying, S.; Hongxing, Y.; Yu, W.; Li, L.H. DAR-based observation and derivation of large-scale wind turbine's wake expansion model downstream of a hill. *Energy* **2022**, *259*, 125051. [CrossRef]
30. Blondel, F.; Cathelain, M. An alternative form of the super-Gaussian wind turbine wake model. *Wind. Energy Sci.* **2020**, *5*, 1225–1236. [CrossRef]
31. Gao, X.; Zhang, S.; Li, L.; Xu, S.; Chen, Y.; Zhu, X.; Sun, H.; Wang, Y.; Lu, H. Quantification of 3D spatiotemporal inhomogeneity for wake characteristics with validations from field measurement and wind tunnel test. *Energy* **2022**, *254*, 124277. [CrossRef]
32. Jensen, N.O. *A Note on Wind Generator Interaction: Citeseer*; Technical Report from the Risø National (LaboratoryRisø-M-2411); Risø National Laboratory: Roskilde, Denmark, 1983.
33. He, R.; Yang, H.; Sun, H.; Gao, X. A novel three-dimensional wake model based on anisotropic Gaussian distribution for wind turbine wakes. *Appl. Energy* **2021**, *296*, 117059. [CrossRef]
34. Gao, X.; Li, B.; Wang, T.; Sun, H.; Yang, H.; Li, Y.; Yu, W.; Zhao, F. Investigation and validation of 3D wake model for horizontal-axis wind turbines based on filed measurements. *Appl. Energy* **2020**, *260*, 114272. [CrossRef]